THE VIRTUAL WHEEL CONCEPT FOR SUPPORTIVE STEERING FEEDBACK DURING ACTIVE STEERING INTERVENTIONS

Avinash Balachandran*
Dynamic Design Laboratory
Department of Mechanical Engineering
Stanford University
Stanford, California 94305
Email: avinashb@stanford.edu

Stephen M. Erlien
J. Christian Gerdes
Dynamic Design Laboratory
Department of Mechanical Engineering
Stanford University
Stanford, California 94305

ABSTRACT

Active steering systems allow for improved vehicle safety and stability through steering interventions that augment a driver's steering command. In a conventional steering system, steering feedback torque depends on the tire forces and corresponding moments that act on the roadwheels. During active steering interventions, there are differences between the driver's command and the actual roadwheel angle. The steering feedback can now be based on either the moments acting on the actual roadwheels or the moments acting on a virtual wheel following the driver's intended steering command. With small interventions, the difference between these two approaches is negligible. However, when the intervention is large (e.g. obstacle avoidance maneuvers), basing handwheel moments on the actual roadwheel position results in a handwheel torque that acts in opposition to the intervention. The virtual wheel concept produces a more supportive, and potentially more intuitive, handwheel torque. This reduces the discrepancy between the driver command and the active steering system in simulation and experiments.

1 INTRODUCTION

Steering authority gives significant control over the lateral dynamics of a vehicle. Active steering augments the driver's steering command either through roadwheel steering corrections or variable steering ratios. This can be used to improve stability and safety by modifying the lateral dynamics of the vehicle. ZF Lenksysteme and BMW AG developed such an active steering system without the loss of mechanical connection from the handwheel to the roadwheel [1]. Steer-by-wire systems also provide a means of creating these active steering interventions. By mechanically decoupling the handwheel from the roadwheel, steer-by-wire systems allow for the actuation of the roadwheels independently from the driver's steering command.

Ackermann et al. [2] described using active steering to aid in various vehicle dynamics control situations. For instance, Switkes et al. [3] used active steering in the lanekeeping task. The magnitude of the active steering interventions for these tasks is typically small. More recently, Anderson et al. [4] and Erlien et al. [5] showed that active steering can be used to maintain an obstacle-free vehicle trajectory. These scenarios, especially obstacle avoidance, typically result in large active steering interventions.

Steering torque feedback at the handwheel, known as steering feel, depends heavily on the tire forces and corresponding moments that act on the roadwheels. Liu and Chang [6] demonstrated that drivers use this feedback to aid the driving task. During an active steering intervention, the driver's intended steering command via the handwheel and the roadwheel angle differs. The steering feedback can now be based on either the moments acting on the actual roadwheels or the moments acting on a virtual wheel following the driver's intended steering command. For small interventions, both approaches result in very similar feedback. However, during a large intervention, basing handwheel moments on the actual roadwheel position results in a handwheel torque that acts in opposition to the intervention.

*Address all correspondence to this author.

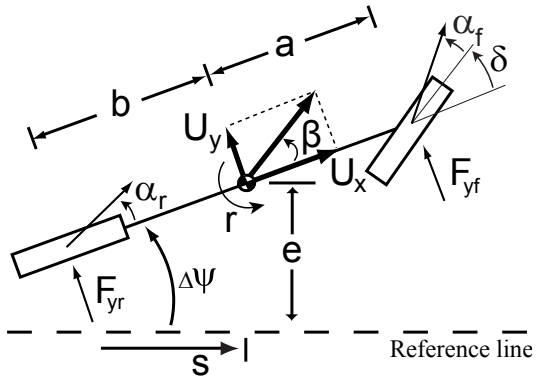

Figure 1. Bicycle model schematic

Using the virtual wheel approach yields torque feedback that is supportive of the intervention.

This paper investigates the interaction between active steering interventions and the usage of the virtual wheel in generating steering torque feedback. Active steering is obtained through a steer-by-wire system. The paper begins by describing the vehicle model that is used for the active steering controller and simulation. As a means of generating steering feedback on a steer-by-wire system, the paper describes a steering feedback model proposed by Balachandran and Gerdes [7]. The paper then incorporates the virtual wheel concept into this model. To investigate the interaction between this model and active steering interventions, large interventions are created using the obstacle avoidance controller proposed by Erlien et al. [5]. The paper then demonstrates, through simulation and experiments, that using the virtual wheel to create supportive handwheel torque reduces the discrepancy between the driver command and the active steering system in simulation and experiments.

2 VEHICLE MODEL

The vehicle model used in this work is a constant speed, planar bicycle model. The vehicle's motion is described by two states: sideslip β and yaw rate r. These are defined in Figure 1 and have the following equations of motion:

$$\dot{\beta} = \frac{F_{yf} + F_{yr}}{mU_x} - r \qquad \dot{r} = \frac{aF_{yf} - bF_{yr}}{I_{zz}} \tag{1}$$

where $F_{y[f,r]}$ is the lateral tire force of the [front, rear] axle, m is the vehicle mass, U_x is the longitudinal velocity in the body fixed frame, I_{zz} is the yaw inertia, and a and b are the distances from the center of gravity to the front and rear axles, respectively.

The simplified Fiala tire model introduced by Pacejka in [8] gives a useful approximation of the non-linear relationship between $F_{y[f,r]}$ and the tire slip angles $\alpha_{[f,r]}$:

$$F_y = \begin{cases} -C_\alpha \tan\alpha + \frac{C_\alpha^2}{3\mu F_z}|\tan\alpha|\tan\alpha \ldots \\ \qquad -\frac{C_\alpha^3}{27\mu^2 F_z^2}\tan^3\alpha, & |\alpha| < \tan^{-1}\left(\frac{3\mu F_z}{C_\alpha}\right) \\ -\mu F_z \operatorname{sgn}\alpha, & \text{otherwise} \end{cases} \tag{2}$$

$$= f_{\text{tire}}(\alpha) \tag{3}$$

where μ is the surface coefficient of friction, F_z is the normal load, and C_α is the tire cornering stiffness.

The tire slip angles, α_f and α_r, can be derived from the kinematics of the vehicle as:

$$\alpha_f = \tan^{-1}\left(\beta + \frac{ar}{U_x}\right) - \delta \tag{4}$$

$$\alpha_r = \tan^{-1}\left(\beta - \frac{br}{U_x}\right) \tag{5}$$

where δ is the steer angle.

The vehicle's position is specified relative to a reference line using three states: heading deviation $\Delta\psi$, lateral deviation e, and distance along the path s as defined in Figure 1.

The equations of motion of these states can be written as:

$$\Delta\dot{\psi} = r \tag{6}$$

$$\dot{e} = U_x \sin(\Delta\psi) + U_y \cos(\Delta\psi) \tag{7}$$

$$\dot{s} = U_x \cos(\Delta\psi) - U_y \sin(\Delta\psi) \tag{8}$$

3 STEERING FEEDBACK MODEL

Figure 2 illustrates the mechanical coupling of the handwheel and the roadwheels in a conventional steering system. In steer-by-wire vehicles, the handwheel is mechanically decoupled from the roadwheels. A force feedback (FFB) steering system can be used in tandem with a steering feedback model to create realistic steering feedback for the driver on a steer-by-wire vehicle. Balachandran and Gerdes [7] proposed a steering feedback model with sufficient complexity to capture the important elements of steering feedback that drivers care about while still being implementable in real-time on a steer-by-wire vehicle. This model depends on the actual roadwheel position of the vehicle. This section briefly introduces this model and further describes the inclusion of the virtual wheel concept into this model.

Due to the FFB steering system ,the handwheel torque felt by a driver (τ_{hw}) has the following dynamics:

$$\tau_{hw} = \tau_{motor} + J_{system}\ddot{\delta}_{hw} + b_{system}\dot{\delta}_{hw} \tag{9}$$

where the handwheel FFB motor torque (τ_{motor}) is commanded, the inherent system inertia (J_{system}) and system damping (b_{system}) are obtained through system identification techniques, and the handwheel angle (δ_{hw}) is a driver input.

3.1 Creating Artificial Steering Feedback

The model emulates the three major torques that make up the steering feedback. They are as follows:

(1) Tire moments
(2) Torques due to inertia and damping
(3) Torque due to power assist

Based on this model, the motor torque (τ_{motor}) is given by:

$$\tau_{\text{motor}} = \tau_{\text{damp}} + \tau_{\text{inertia}} + K\tau_{\text{assisted tire moment}} \tag{10}$$

where the damping torque (τ_{damp}) and inertia torque (τ_{inertia}) modify the inherent damping and inertia of the steering system and the assisted tire moment ($\tau_{\text{assisted tire moment}}$) represents the combined effect of the aligning moment, jacking torque and power assist. These are discussed briefly below. The tire moment gain (K) accounts for the transmission of moments from the tire to the handwheel and varies for different steering systems, suspension geometries and steering ratios.

3.1.1 Damping Torque (τ_{damp}) Damping torque modifies the effect of the inherent system damping (b_{system}) on steering feedback. It is created using the following model:

$$\tau_{\text{damp}} = -\Delta b\dot{\delta} \tag{11}$$

where the change in damping (Δb) to the system is chosen.

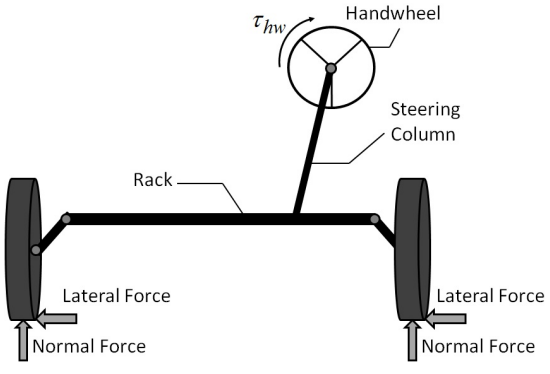

Figure 2. Conventional steering system

3.1.2 Inertia Torque (τ_{inertia}) Inertia torque modifies the effect of the inherent system inertia (J_{system}) on steering feedback. It is created using the following model:

$$\tau_{\text{inertia}} = -\Delta J\ddot{\delta} \tag{12}$$

where the change in inertia (ΔJ) to the system is chosen.

3.1.3 Aligning Moment (τ_{align}) Front tire forces and their resulting moments have a large effect on steering feedback. The effect that the front *lateral* tire forces (F_{yf}) have on steering feedback is recreated via the aligning moment, which dominates steering feedback at higher speeds. Aligning moment is approximated as the product of the front lateral tire forces and the total trail of the vehicle as shown:

$$\tau_{\text{align}} = -F_{\text{yf}}(t_{\text{m}} + t_{\text{p}}) \tag{13}$$

where t_{m} is the mechanical trail and t_{p} is the pneumatic trail of the vehicle.

The front tire force is obtained using (2) where the surface coefficient of friction (μ), normal load (F_{z}), and tire cornering stiffness (C_{α}) are all assumed to be known.

For simplicity, the mechanical trail (t_{m}) is assumed to be constant and the pneumatic trail (t_{p}) is modeled as a decreasing linear function of slip angle as introduced by Hsu and Gerdes [9]:

$$t_{\text{p}} = t_{\text{p0}} - \text{sgn}(\alpha_{\text{f}})\frac{t_{\text{p0}}C_{\alpha\text{f}}}{3\mu F_{\text{zf}}}\tan(\alpha_{\text{f}}) \tag{14}$$

where the pneumatic trail at zero front slip angle (t_{p0}), surface coefficient of friction (μ), front normal tire force (F_{zf}) and front tire cornering stiffness ($C_{\alpha\text{f}}$) are assumed to be known. This simplification reduces the number of tuning parameters needed. The front slip angle (α_{f}) is obtained from the measured vehicle's sideslip (β), yawrate (r), longitudinal speed (U_{x}) and steer angle (δ) using (4).

3.1.4 Jacking Torque (τ_{jack}) The front *normal* tire forces (F_{zf}) affect the steering feedback via the jacking torque. Jacking torque creates the centering feedback for a driver at low speeds. A spring model gives a useful approximation of jacking torque and captures this important centering effect in a simple model. In a production vehicle, the steering system typically has a deadband in which the stiffness is lower. A two spring constant model allows the deadband characteristics to be incorporated into the algorithm.

$$\tau_{\text{jack}} = \begin{cases} -k_{\text{db}}\delta & |\delta| \leq \delta_{\text{db}} \\ -k_{\text{jack}}\delta - k_{\text{db}}(\text{sgn}(\delta) * \delta_{\text{db}}) & |\delta| > \delta_{\text{db}} \end{cases} \tag{15}$$

where the steering deadband (δ_{db}), deadband spring constant (k_{db}) and jacking torque spring constant (k_{jack}) are chosen. The resultant τ_{jack} given by this function is continuous. The two spring constants represent the different stiffnesses due to the steering deadband region.

3.1.5 Power Assist Effect In modern power steering systems, drivers receive an assistive torque counteracting the total front tire moment to aid them in turning the roadwheels. This torque factors into the steering feedback. Ryu and Kim demonstrated that the effect of this assistive torque on the resultant steering feedback is that a smaller fraction of the total front tire moment is included in the steering feedback [10]. Using the expressions for aligning moment and jacking torque obtained earlier, the total front tire moment can be approximated by:

$$\tau_{\text{tire moment}} \approx \tau_{\text{jack}} + \tau_{\text{align}} \tag{16}$$

The fraction of the total front tire moment felt by the driver is then modeled as a weighting function (W_f) that depends on front slip angle. The resultant assisted total front tire moment is given as:

$$\tau_{\text{assisted tire moment}} = \tau_{\text{tire moment}} W_{\text{f}} \tag{17}$$

Building on the work of Ryu and Kim, the weighting function (W_{f}) is modeled as a Gaussian function and is given by:

$$W_{\text{f}} = e^{\frac{-\alpha_{\text{f}}^2}{2\sigma_{\text{ps}}^2}}(1-\gamma) + \gamma \tag{18}$$

where the front slip angle (α_{f}) is known while the standard deviation (σ_{ps}) and lower limit (γ) for the weighting function are selected to create the desired power steering effect. A typical weighting function is illustrated in Figure 3.

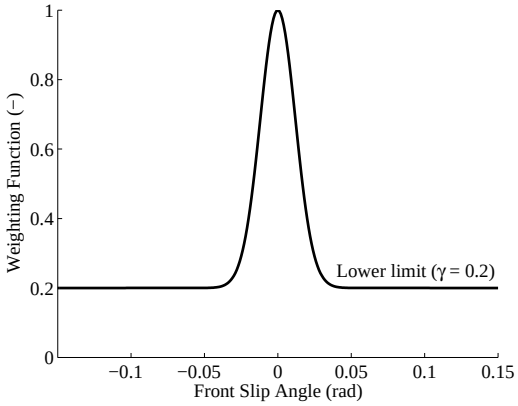

Figure 3. Power assist weighting function

3.2 Incorporating the Virtual Wheel

When a vehicle experiences an active steering intervention, the roadwheel angle differs from the desired steering command obtained from the handwheel. The steering feedback can now be based on either the moments acting on the actual roadwheels or the moments that would act on roadwheels had they followed the driver's intended steering command (known as the virtual wheel concept). The model presented above can incorporate both these options. If feedback based on the moments acting on the actual roadwheels is desired, the steer angle used in Equations (4), (11), (12) and (15) to obtain front slip angle, damping torque, inertia torque and jacking torque respectively would be the actual roadwheel angle (δ_{rw}):

$$\delta = \delta_{\text{rw}} \tag{19}$$

If the virtual wheel concept is desired, then the steer angle used in these equations would be the driver's intended steer angle based on the handwheel angle:

$$\delta = \frac{\delta_{\text{hw}}}{\text{SteeringRatio}} \tag{20}$$

4 OBSTACLE AVOIDANCE CONTROLLER

To investigate the interaction between active steering interventions and the usage of the virtual wheel in generating steering torque feedback, a controller which creates large interventions is required. Large interventions result in a bigger difference between the feedback using virtual wheel and the feedback using the actual roadwheel position. Since obstacle avoidance controllers generally result in large active steering interventions, this paper uses the obstacle avoidance controller developed by Erlien and Gerdes [5].

This controller shares control with a human driver using safe driving envelopes. Vehicle handling limits define the stable han-

dling envelope while obstacles and road boundaries in the environment define the environmental envelope. A Model Predictive Control (MPC) scheme determines if the driver's current steering command allows for a safe vehicle trajectory within these two safe driving envelopes, intervening when such a trajectory does not exist. This controller is briefly described in this section.

4.1 MPC Vehicle Model

The vehicle model used in the online MPC controller is a linearization of the vehicle model presented in Section 2. Although this model assumes constant speed, in practice, the measured vehicle speed is used at each execution of the MPC controller and only assumed constant over the prediction horizon. The input to this vehicle model is F_{yf}; therefore, the controller computes an optimal front tire force which is then mapped to δ_{rw} using (3) and (4):

$$\delta_{\mathrm{rw}} = \beta + \frac{ar}{U_{\mathrm{x}}} - f_{\mathrm{tire}}^{-1}\left(F_{\mathrm{yf}}\right) \tag{21}$$

where f_{tire}^{-1} is computed numerically.

Use of F_{yf} as the model input enables explicit consideration of the non-linear dynamics of the front tires. For the rear tires, which cannot be steered, a linearization of non-linear tire model (3) at a nominal rear tire slip angle, $\bar{\alpha}_{\mathrm{r}}$, models rear tire force, F_{yr}, as an affine function of α_{r}:

$$F_{\mathrm{yr}} = \bar{F}_{\mathrm{yr}} - \bar{C}_{\bar{\alpha}_{\mathrm{r}}}(\alpha_{\mathrm{r}} - \bar{\alpha}_{\mathrm{r}}) \tag{22}$$

where $\bar{F}_{\mathrm{yr}} = f_{\mathrm{tire}}\left(\bar{\alpha}_{\mathrm{r}}\right)$ and $\bar{C}_{\bar{\alpha}_{\mathrm{r}}}$ is the equivalent cornering stiffness at $\bar{\alpha}_{\mathrm{r}}$. In the near term of the prediction horizon, this rear tire model is linearized around the measured rear tire slip angle, α_{r}, as was done by Beal and Gerdes [11], which enables accurate prediction of vehicle state propagation in the near term. In the remainder of the horizon, a linear tire model with $\bar{\alpha}_{\mathrm{r}} = 0$ is used.

Small angle approximations give linear expressions for non-linear tire slip equations (4) and (5). Equations (7) and (8) for the positional states of the vehicle can be similarly simplified as:

$$\dot{e} \approx U_{\mathrm{x}}\Delta\psi + U_{\mathrm{x}}\beta \tag{23}$$

$$\dot{s} \approx U_{\mathrm{x}} - U_{\mathrm{x}}\beta\Delta\psi \approx U_{\mathrm{x}} \tag{24}$$

using small angle assumptions for $\Delta\psi$ and β. With these simplifying assumptions, a discrete, time-varying vehicle model can be expressed as:

$$x^{(k+1)} = A_{\bar{\alpha}_{\mathrm{r}},t_{\mathrm{s}}}^{(k)} x^{(k)} + B_{\bar{\alpha}_r,t_s}^{(k)} F_{\mathrm{yf}}{}^{(k)} + d_{\bar{\alpha}_r,t_s}^{(k)} \tag{25}$$

where $x = \begin{bmatrix}\beta & r & \Delta\psi & s & e\end{bmatrix}^T$, k is a time step index, subscript $\bar{\alpha}_{\mathrm{r}}$ denotes linearization of the rear tire model around rear slip angle $\bar{\alpha}_{\mathrm{r}}$, and subscript t_{s} denotes discretization of the vehicle model using time step length t_{s}.

4.2 Stable Handling Envelope

Originally presented by Beal and Gerdes, the stable handling envelope defines limits on the states describing the vehicle's motion as illustrated in Figure 4. This envelope reflects the maximum capabilities of the vehicle's tires so at any point within this envelope, there exists a steering command to safely remain inside, ensuring stability [11].

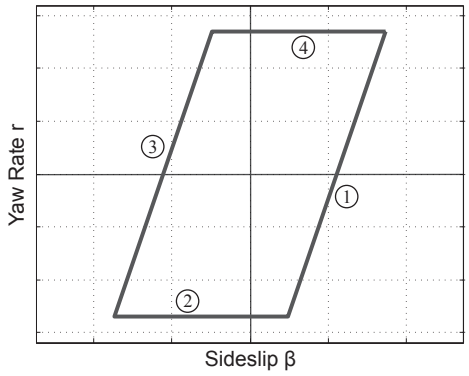

Figure 4. Stable handling envelope

The maximum steady-state yaw rate defines bounds (2) and (4) in Figure 4, while the rear slip angle at which lateral force saturates serves as the basis for bounds (1) and (3). The desire to restrain the vehicle states within the stable handling envelope will be compactly expressed as the inequality:

$$\left|H_{\mathrm{sh}} x^{(k)}\right| \leq G_{\mathrm{sh}} \tag{26}$$

where subscript sh indicates the stable handling envelope.

4.3 Environmental Envelope

The environmental envelope consists of a set of collision free tubes along the reference line like the two illustrated in Figure 5. To avoid collision with the environment, the vehicle's trajectory must be fully contained within any one of these tubes. Each tube defines time-varying constraints on the lateral devia-

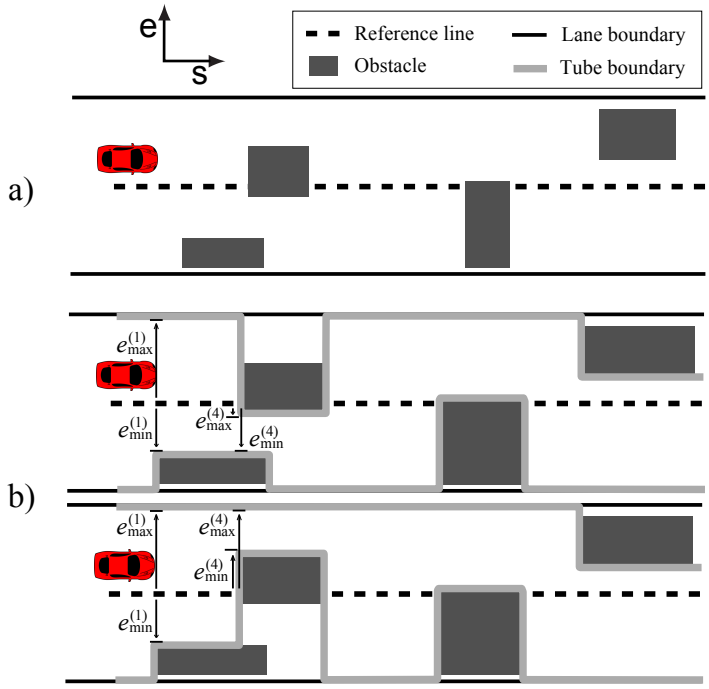

Figure 5. The environmental envelope is a representation of a) a collection of obstacles along the reference line using b) tubes (two of them in this example) which define a maximum $(e^{(k)}_{\max})$ and minimum $(e^{(k)}_{\min})$ lateral deviation from the reference line at each time step, k.

tion of the vehicle from the reference line:

$$e^{(k)} \leq e^{(k)}_{\max} - \frac{1}{2}d - d_{\text{buffer}} \tag{27}$$

$$e^{(k)} \geq e^{(k)}_{\min} + \frac{1}{2}d + d_{\text{buffer}} \tag{28}$$

where $e^{(k)}_{\max}$ and $e^{(k)}_{\min}$ indicate the lateral deviation bounds for time step k, d is the vehicle's width, and d_{buffer} specifies a preferred minimum distance between obstacles and the vehicle to ensure driver comfort.

Inequalities (27) and (28) can be compactly expressed as:

$$H_{\text{env}}x^{(k)} \leq G^{(k)}_{\text{env}} \tag{29}$$

where subscript env indicates the environmental envelope. A vehicle trajectory is collision free throughout the prediction horizon if and only if it satisfies inequality (29) for all k for any *one* tube in the environmental envelope. In this paper, the environments that are considered can be represented using only one tube; however, the authors previously published a method for handling multi-tube environments and generating these tubes in real-time [5].

4.4 MPC Formulation

The controller's objectives can be expressed as an optimization problem to be evaluated over a finite prediction horizon:

$$\begin{aligned}
\text{minimize} \quad & \left|F_{\text{yf,driver}} - F^{(0)}_{\text{yf,opt}}\right| && \text{(30a)}\\
& + \sum_k \gamma^{(k)} \left|\left|F^{(k)}_{\text{yf,opt}} - F^{(k-1)}_{\text{yf,opt}}\right|\right|_2 && \text{(30b)}\\
\text{subject to} \quad & x^{(k+1)} = A^{(k)}_{\tilde{\alpha}_r,t_s}x^{(k)} + B^{(k)}_{\tilde{\alpha}_r,t_s}F^{(k)}_{\text{yf,opt}} + d^{(k)}_{\tilde{\alpha}_r,t_s} && \text{(30c)}\\
& \left|F^{(k)}_{\text{yf,opt}}\right| \leq F_{\text{yf,max}} && \text{(30d)}\\
& \left|H_{\text{sh}}x^{(k+1)}\right| \leq G_{\text{sh}} && \text{(30e)}\\
& H_{\text{env}}x^{(k+1)} \leq G^{(k+1)}_{\text{env}} && \text{(30f)}\\
& \left|F^{(k)}_{\text{yf,opt}} - F^{(k-1)}_{\text{yf,opt}}\right| \leq F^{(k)}_{\text{yf,max slew}} && \text{(30g)}
\end{aligned}$$

where $k = 0 \ldots 29$ and the variables to be optimized are the optimal input trajectory ($F_{\text{yf,opt}}$). As is commonly done in MPC, only the optimal input for the first step into the prediction horizon, $F^{(0)}_{\text{yf,opt}}$, is applied to the vehicle, and optimization problem (30) is re-solved at the next time step.

A tunable parameter in this optimization is γ, which establishes the trade-off between a smooth input trajectory (30b) and matching the driver's present steering command (30a). Cost term (30a) uses the l_1 norm as a convex approximation to the objective of *identically matching* the driver's command where $F_{\text{yf,driver}}$ is the front tire force corresponding to the driver's hand wheel , δ_{hw}. Tire model (3) provides the mapping from δ_{hw} to $F_{\text{yf,driver}}$:

$$F_{\text{yf,driver}} = f_{\text{tire}}\left(\beta + \frac{ar}{U_x} - \delta_{\text{hw}}\right) \tag{31}$$

Constraint (30d) reflects the maximum force capabilities of the front tires and (30g) reflects the slew rate limit of the steer-by-wire system. Constraints (30e) and (30f) enforce the stable handling and environmental envelopes, respectively. In practice, these constraints are softened with slack variables to ensure optimization (30) is always feasible.

The prediction horizon used in optimization (30) uses different length time steps in the near and long terms of the horizon to consider obstacles in the long term without compromising the prediction of vehicle states in the near term. Table 1 gives the values of parameters in these two portions of the prediction horizon.

CVXGEN [12] is used to leverage the significantly sparse structure of convex optimization problem (30) to produce an efficient solver for real-time implementation [13].

5 INTERACTION BETWEEN STEERING TORQUE FEEDACK AND ACTIVE STEERING

During an active steering intervention, the driver's steering command via the handwheel differs from the actual roadwheel position. The steering torque feedback can now either be based on the moments acting on the actual roadwheels or the moments acting on a virtual wheel following the driver's intended steering command. This section discusses the impact of both these approaches through simulation.

5.1 Simulation

The effect of both these feedback approaches with an active steering intervention for obstacle avoidance can be studied using a simple non-linear vehicle simulation based on the vehicle model presented in Section 2. The simulation scenario used in this paper illustrates an inattentive driver who veers into an obstacle at the side of the road. The driver is initially modeled as slowly increasing the steering angle so that he veers into the obstacle. Once the active steering intervention begins, the steering torque varies quickly and, sometimes, drastically. Suzuki [14] showed that different drivers react differently to steering torque feedback with some acting exactly the opposite as others. In order to model the driver during the intervention, this simulation uses a simple spring damper model of the passive arm and steering dynamics developed by Pick and Cole [15]:

$$J_{\text{driver}}\ddot{\delta}_{\text{hw}} + b_{\text{driver}}\dot{\delta}_{\text{hw}} + k_{\text{driver}}\delta_{\text{hw}} = \tau_{\text{hw}} \tag{32}$$

where the driver's arm and steering inertia (J_{driver}), damping (b_{driver}) and spring constant (k_{driver}) are determined through averaging measurements taken over eight test subjects. This model acts as a simple abstraction for a driver who simply allows his arm and steering system dynamics to dictate his handwheel angle (i.e. passive driver).

Table 1. Prediction Horizon Parameters

Parameter	Near Term Horizon	Long Term Horizon
k	0...9	10...29
t_s	0.01 [s]	0.2 [s]
γ	30	1.5
$F_{\text{yf,max slew}}$	0.2 [kN]	5 [kN]
$\bar{\alpha}_r$	α_r	0

5.1.1 Simulation Results

Figure 6 illustrates the simulation scenario of an inattentive driver who veers into an obstacle (the red boxes) at the side of the road. The vertical dotted cyan line illustrates when the active steering intervention begins. When the active steering intervention occurs (i.e. 3.1 - 4.1 [s]), the steering torque acts in opposition to the intervention. It causes the driver to turn the handwheel in the opposite direction of the intervention. The driver turns the handwheel left while the vehicle's active steering intervention is moving the vehicle to the right. This increases the discrepancy between the driver and the controller and results in the active steering system deviating further from the driver's command. These effects enhance the disconnection between the driver's actions and the vehicle's motion.

Figure 7 illustrates the same simulation scenario as Figure 6 but with the virtual wheel concept implemented. The steering feedback now has the same sign as the actual roadwheel command during the intervention (i.e. 3.1 - 4.3 [s]). This steering torque acts to support the intervention. The simple passive driver model shows that the driver's steering command now indeed moves in the same direction as the actual roadwheel angle. Therefore, the driver's actions now have a smaller deviation from the active steering system.

5.1.2 Discussion

The reason that the virtual wheel results in supportive steering torque feedback is that the feedback

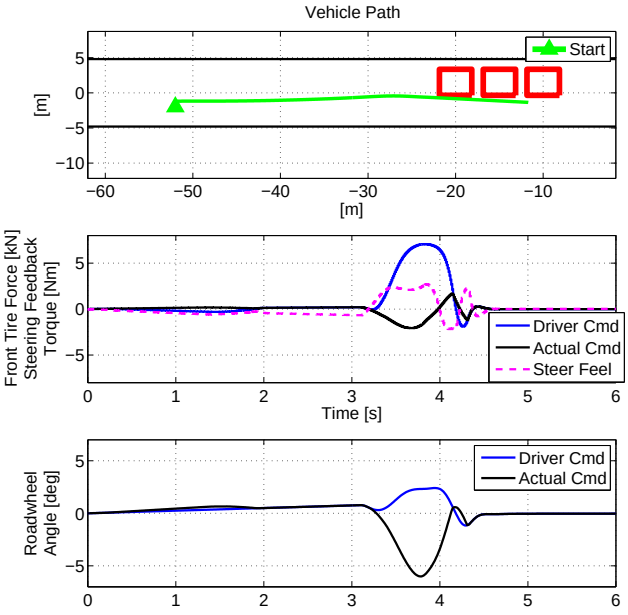

Figure 6. Simulation: Feedback without the virtual wheel

contains a large aligning moment component. During an active steering intervention, the controller either increases or decreases the actual front lateral tire force (F_{yf}) beyond the driver's intended command. Based on Equation (13), the actual roadwheel aligning moment has the opposite sign to the front lateral tire force. This causes the active steering intervention to always act in a manner that results in the actual aligning moment opposing it. If the actual roadwheel position rather than the virtual wheel is used to the generate the feedback, the driver feels this actual aligning moment component in the steering feedback and acts to turn the handwheel to oppose the intervention.

For example, if the intervention commands a more positive tire force than the driver's command, the aligning moment based on the actual roadwheel position would be more negative than the aligning moment based on the driver's intended roadwheel angle (i.e. the virtual wheel). Using feedback based on the actual roadwheel position results in the driver getting a 'heavier' feel which tends to cause the driver to reduce the his commanded tire force in opposition to the intent of the steering intervention. This problem becomes more pronounced when the intervention results in a flip in the sign of the tire force between the driver's command and the intervention. For example. when the driver commands a positive tire force and the intervention commands a negative tire force, using the actual roadwheel position for feedback results in a positive torque feedback that causes the driver to turn more to the left and increases the driver commanded tire force. Once again, this is in opposition to the intent of the intervention.

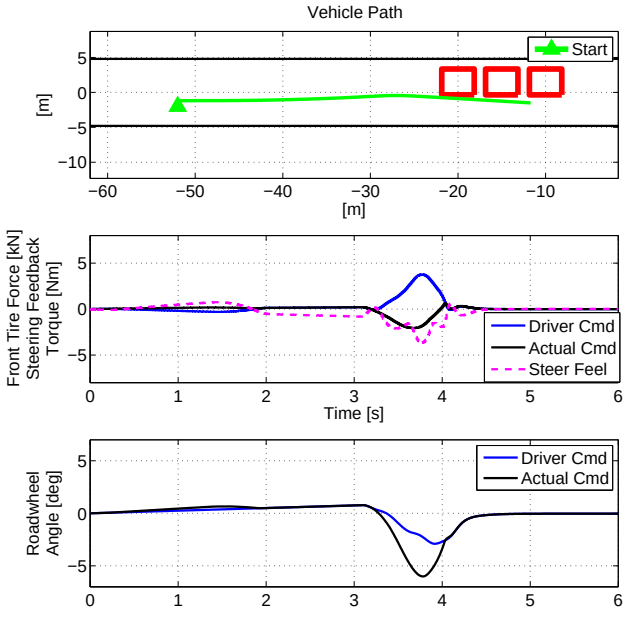

Figure 7. Simulation: Feedback with virtual wheel

Using the virtual wheel to generate the feedback mitigates these problems. The feedback now is based on the driver commanded tire force and the corresponding aligning moment. If the intervention results in a larger tire force than the driver command, the feedback will now not result in a 'heavier' feel that causes the driver to act against the intervention. Similarly, if the intervention results in a tire force that changes sign from the driver command, using the virtual wheel results in feedback that causes the driver to turn to change the sign of the driver command as well. In this way, the using the virtual wheel to create feedback results in the driver obtaining supportive steering feedback during active steering interventions.

6 EXPERIMENTAL VALIDATION

Experiments run on the steer-by-wire vehicle, X1 (illustrated in Figure 8) confirmed these simulations. X1 is a true steer-by-wire vehicle with independent steering motors on each wheel and no steering rack or torsion bar. A FFB steering system generates artificial steering feedback at the handwheel. Precise encoders obtain the handwheel angle and roadwheel angle while the roadwheel angle derivative is approximated by differencing the encoder signal.

X1 uses an integrated Global Positioning System (GPS) and Inertia Measurement System (INS) to obtain the yawrate (r), sideslip (β) and longitudinal speed (U_x) of the vehicle. Based on (4), the front slip angle (α_f) can be calculated from this information. The motor torque (τ_{motor}) is then fed to the motor that is part of the FFB steering system on the vehicle. A dSPACE MicroAutoBox II (DS1401) interfaces with the subsystems of the vehicle at a rate of 500 [Hz] with the model predictive controller implemented on a single core of an i7 processor utilizing MATLABs real-time toolbox at a rate of 100 [Hz].

6.1 Test Scenario

The experiment involves the vehicle being intentionally driven towards the left road boundary. Based on the controller described in Section 4, when the vehicle's future trajectory violates the road boundary, the active steering engages to prevent the violation. After each time the driver drives towards the road boundary and the active steering intervention engages, the driver drives away from the boundary and repeats the process a few meters later. This is done three times in each data set. The experiment was performed on an asphalt road with friction coefficient (μ) of about 0.85.

6.2 Experimental Results

Figure 9 shows the data from the test without the virtual wheel. The driver drives into the left road edge three times at around 11 [s], 14 [s] and 17.5 [s]. At each of these times, the

steering feedback acts in the opposite direction to the actual roadwheel command. Therefore, the feedback opposes the intervention. This increases the discrepancy between the driver's command and the active steering system. There is a disconnection between the driver's actions and the vehicle's motion. This also results in the driver being pulled into the road boundary.

Figure 10 illustrates a similar test but with the virtual wheel concept implemented. Once again the driver drives into the left road edge three times at around 7.5 [s], 10 [s] and 12.5 [s]. At each of these times, the steering feedback acts in the same direction to the actual roadwheel command. The feedback now supports the intervention. Instead of being pulled into the road boundary as before, the steering feedback acts to push the driver away from the boundary and maintain a safe trajectory. This reduces the discrepancy between the driver's command and the active steering system (as seen in the bottom plot). Now, there is a much smaller disconnection between the driver's actions and the vehicle's motion.

Figure 8. X1 Steer-by-wire vehicle

7 CONCLUSION

This paper investigates the interaction between steering feedback and large active steering interventions. Steering feedback that is based on the actual roadwheel position results in handwheel torque that opposes the intervention. This leads to a large discrepancy between the driver's command and the active steering controller. By introducing the virtual wheel concept, this paper proposes to use the driver's intended aligning moment command rather than the actual aligning moment for steering torque feedback. This technique allows for a realistic steering feedback when there is no active steering intervention as the driver's intended aligning moment is the same as the actual aligning moment. During a large active steering intervention, this technique results in steering feedback that supports the intervention. Simulation and experiments demonstrate that this

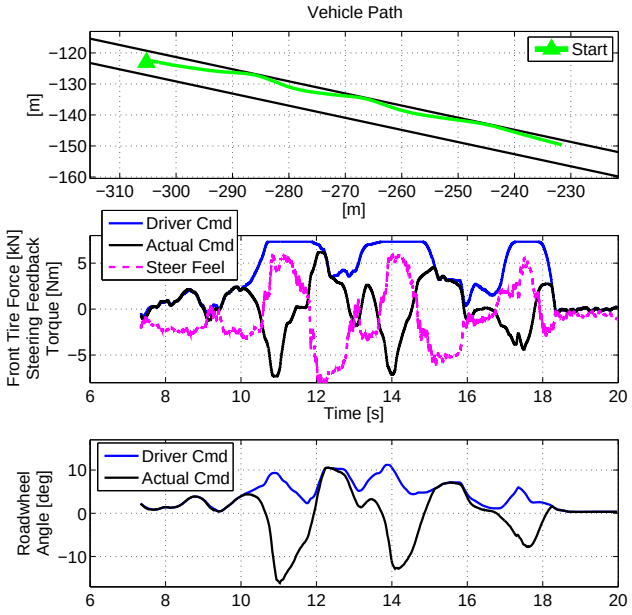

Figure 9. Experiment: Feedback without virtual wheel

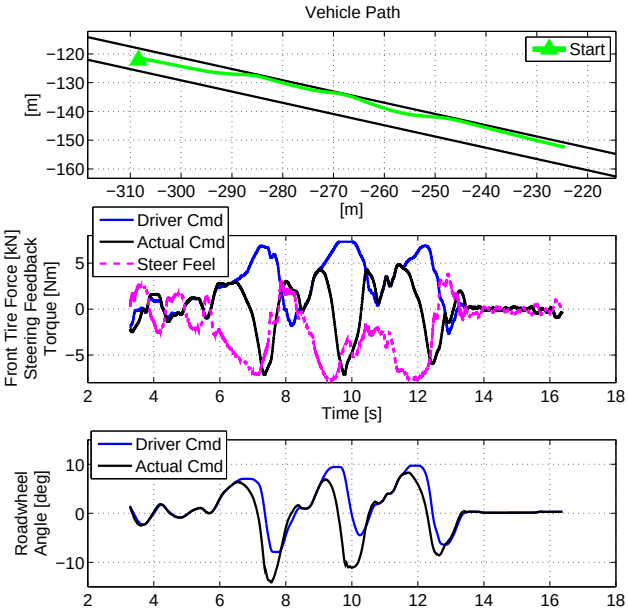

Figure 10. Experiment: Feedback with virtual wheel

reduces the discrepancy between the driver's command and the active steering system.

ACKNOWLEDGMENT

The authors would like to thank the NISSAN MOTOR Co., Ltd. and project team members Susumu Fujita and Hikaru Nishira for supporting this research.

REFERENCES

[1] Koehn, P., and Eckrich, M., 2004. "Active steering - The BMW approach towards modern steering technology". *SAE International 2004-01-1105*, Mar.

[2] Ackermann, J., Odenthal, D., and Bunte, T., 1999. "Advantages of active steering for vehicle dynamics control". *Proceedings of 32nd ISATA, Automotive Mechatronics Design and Engineering*, pp. 263–270.

[3] Switkes, J. P., Rossetter, E. J., Coe, I. A., and Gerdes, J. C., 2006. "Handwheel force feedback for lanekeeping assistance: combined dynamics and stability". *ASME Journal of Dynamic Systems, Measurement, and Control,* ***128***(3), p. 532.

[4] Anderson, S. J., Karumanchi, S. B., and Iagnemma, K., 2012. "Constraint-based planning and control for safe, semi-autonomous operation of vehicles". In 2012 IEEE Intelligent Vehicles Symposium, IEEE, pp. 383–388.

[5] Erlien, S. M., Fujita, S., and Gerdes, J. C., 2013. "Safe driving envelopes for shared control of ground vehicles". In 7th IFAC Symposium on Advances in Automotive Control, pp. 831–836.

[6] Liu, A., and Chang, S., 1995. "Force feedback in a stationary driving simulator". *1995 IEEE International Conference on Systems, Man and Cybernetics,* ***2***(2), pp. 1711–1716.

[7] Balachandran, A., and Gerdes, J. C., 2014. "Designing Steering Feel for Steer-by-Wire Vehicles Using Objective Measures". *IEEE/ASME Transactions on Mechatronics, DOI: 10.1109/TMECH.2014.2324593,* ***In Press***.

[8] Pacejka, H., 2012. *Tire and Vehicle Dynamics*, butterworth ed.

[9] Hsu, Y. H. J., and Gerdes, J. C., 2006. "A feel for the road: A method to estimate tire parameters using steering torque". In International Symposium on Advanced Vehicle Control.

[10] Ryu, J., and Kim, H. S., 1999. "Virtual environment for developing electronic power steering and steer-by-wire systems". In Intelligent Robots and Systems, 1999. IROS'99. Proceedings. 1999 IEEE/RSJ International Conference on, Vol. 3, IEEE, pp. 1374–1379.

[11] Beal, C. E., and Gerdes, J. C., 2013. "Model predictive control for vehicle stabilization at the limits of handling". *IEEE Transactions on Control Systems Technology,* ***21***(4), July, pp. 1258–1269.

[12] Mattingley, J., and Boyd, S., 2012. "CVXGEN: a code generator for embedded convex optimization". *Optimization and Engineering,* ***13***(1), pp. 1–27.

[13] Mattingley, J., Wang, Y., and Boyd, S., 2010. "Code generation for receding horizon control". In 2010 IEEE International Symposium on Computer-Aided Control System Design (CACSD), pp. 985–992.

[14] Suzuki, K., 2002. "Analysis of driver's steering behavior during auditory or haptic warnings in lane departure situations". *Proceedings of the International Symposium on Advanced Vehicle Control (AVEC),* ***JSAE 20024***.

[15] Pick, A. J., and Cole, D. J., 2008. "A Mathematical Model of Driver Steering Control Including Neuromuscular Dynamics". *ASME Journal of Dynamic Systems, Measurement, and Control,* ***130***(3), p. 031004.